

## Comparison of nucleon-nucleon potential models in a full-folding description of elastic scattering

H. F. Arellano

*Department of Physics and Astronomy, University of Georgia, Athens, Georgia 30602*

F. A. Brieva

*Department of Physics and Astronomy, University of Georgia, Athens, Georgia 30602  
and Departamento de Física, Facultad de Ciencias Físicas y Matemáticas, Universidad de Chile,  
Casilla 487-3, Santiago, Chile*

W. G. Love and K. Nakayama

*Department of Physics and Astronomy, University of Georgia, Athens, Georgia 30602*

(Received 5 December 1990)

The sensitivity of proton-nucleus elastic scattering to different nucleon-nucleon effective interactions is studied within the framework of the nonrelativistic full-folding model. Calculations of the nucleon-nucleus optical potential are made using the free nucleon-nucleon  $t$ -matrices generated from the Bonn, Paris, Hamada-Johnston, and Melbourne nucleon-nucleon potentials, whose full off-shell behavior is treated explicitly. Applications are made to  $p + {}^{40}\text{Ca}$  elastic scattering at energies of 200, 300, and 400 MeV within the full-folding framework. Calculations using the on-shell  $t\rho$  model have been made for comparison. Both full-folding and  $t\rho$  results show comparable sensitivity to the particular choice of effective interaction, demonstrating the importance of a realistic description of the nucleon-nucleon interaction both on and off the energy shell.

Recent developments in intermediate-energy nucleon-nucleus scattering have demonstrated<sup>1-3</sup> the importance of including explicitly the off-shell behavior of the nucleon-nucleon ( $NN$ ) effective interaction. In particular, accurate treatments of these off-shell degrees of freedom in a nonrelativistic full-folding optical potential have provided<sup>1-3</sup> a substantial improvement in the description of nucleon-nucleus ( $NA$ ) elastic-scattering data when compared with alternative approximations to the optical potential which have an on-shell factorized " $t\rho$ " structure in momentum space. These findings demonstrate that nucleon-nucleus elastic scattering is sensitive to the approximations made in treating the off-shell behavior of the  $NN$  effective interaction. In particular, nucleon-nucleus scattering is sensitive to the design of models of the  $NN$  potential and to its intrinsic off-shell properties as determined by the Lippmann-Schwinger or Schrödinger equation. In the present work, we address the degree of sensitivity of the full-folding calculations to the use of alternative  $NN$  potentials. A knowledge of the level of sensitivity to different  $NN$  potential models is critical for understanding and estimating the associated uncertainties and limitations in microscopic calculations of nuclear structure and nuclear reactions.

Although full-folding and approximate full-folding results have been reported previously using different  $NN$  potentials,<sup>1-3</sup> meaningful comparisons are difficult because different approximations have been used by the different groups and these approximations are known to be nonequivalent. In order to compare the use of different  $NN$  potentials directly, we consider four distinct

potentials within a common full-folding framework. The  $NN$  potentials we consider are the Paris potential,<sup>4</sup> the Bonn momentum-space one-boson-exchange potential (OBEPQ),<sup>5</sup> the Hamada-Johnston<sup>6</sup> (HJ) potential, and the recently developed Melbourne<sup>7</sup> potential.

Each of the above potentials is realistic in the sense that they describe  $NN$  scattering data below about 350 MeV. The Paris and Bonn potentials are currently the most widely used descriptions of the  $NN$  interaction and are based primarily on the underlying hadronic degrees of freedom (meson-exchange models). In particular, the medium- and long-range parts of the Paris interaction are described in terms of  $\pi$ -,  $2\pi$ -, and  $\omega$ -exchange terms. Its short-range ( $r \lesssim 0.8$  fm) part is represented by a phenomenological soft core.<sup>4</sup> In the present calculations, we use the Yukawa parametrization<sup>4</sup> of the Paris potential. The Bonn potential considered<sup>5</sup> is a one-boson-exchange potential (OBEP) containing form factors which regularize the potential at short distances. The HJ potential is primarily phenomenological with a hard core in all states; its long-range part is constrained by the one-pion-exchange process. The Melbourne potential is an empirical model in which boson-exchange form factors ( $\pi$ ,  $2\pi$ ,  $\rho$ , and  $\omega$ ) are multiplied by parametric functions of the relative  $NN$  momenta; these functions are determined by fitting  $NN$  scattering data up to 400 MeV.

The details of the full-folding model calculations are given in Ref. 1 and are used with each of the  $t$  matrices generated by the above potentials so that here we indicate only the most essential elements. In the absence of medium corrections to the  $NN$  effective interaction and when

the single-particle energies of the bound nucleons may be approximated by an average value  $\epsilon$  ( $\epsilon \approx -25$  MeV in the case of  $^{40}\text{Ca}$ ), the full-folding optical potential for proton-nucleus scattering can be expressed in terms of the free  $t$  matrix ( $t$ ) and the ground-state mixed density  $\rho$  by<sup>1</sup>

$$U(\mathbf{k}', \mathbf{k}; E) = \int d\mathbf{P} \rho(\mathbf{P} + \frac{1}{2}\mathbf{q}, \mathbf{P} - \frac{1}{2}\mathbf{q}) \langle \boldsymbol{\kappa}' | t(z) | \boldsymbol{\kappa} \rangle, \quad (1)$$

where  $\mathbf{q} = \mathbf{k} - \mathbf{k}'$  and  $\rho$  is given in terms of occupied single-particle states  $\varphi_\alpha$  by

$$\rho(\mathbf{P} + \frac{1}{2}\mathbf{q}, \mathbf{P} - \frac{1}{2}\mathbf{q}) = \sum_\alpha \varphi_\alpha^\dagger(\mathbf{P} + \frac{1}{2}\mathbf{q}) \varphi_\alpha(\mathbf{P} - \frac{1}{2}\mathbf{q}). \quad (2)$$

The momentum and energy variables in the  $t$  matrix are defined by

$$\begin{aligned} \boldsymbol{\kappa}' &= \frac{1}{2}(\mathbf{K} - \mathbf{P} - \mathbf{q}), \\ \boldsymbol{\kappa} &= \frac{1}{2}(\mathbf{K} - \mathbf{P} + \mathbf{q}), \\ z &= E + \epsilon - \frac{(\mathbf{P} + \mathbf{K})^2}{2M}, \\ \mathbf{K} &= \frac{1}{2}(\mathbf{k} + \mathbf{k}'). \end{aligned} \quad (3)$$

The integration is over the mean momentum ( $\mathbf{P}$ ) of the struck nucleon before and after collision. The momentum  $\boldsymbol{\kappa}$  ( $\boldsymbol{\kappa}'$ ) represents the incoming (outgoing) relative momentum in the  $NN$  center of mass and  $z$  represents the propagating energy in the same system. These three variables are not constrained to be on shell. The free  $t$  matrix is calculated off shell from the different  $NN$  potentials by solving either the Lippmann-Schwinger integral equation or the corresponding Schrödinger equation.<sup>1</sup>

A critical feature of the optical potential in the full-folding approach is the inclusion of off-shell effects consistently as allowed by the momentum distribution of the mixed density  $\rho$ . In Fig. 1, we show a plot of  $P^2\rho(\mathbf{P} + \frac{1}{2}\mathbf{q}, \mathbf{P} - \frac{1}{2}\mathbf{q})$  for  $^{40}\text{Ca}$  as a function of  $\mathbf{P}$  and  $\mathbf{q}$ ; the result depends very weakly<sup>1</sup> on the angle between  $\mathbf{P}$  and  $\mathbf{q}$ . From this figure it becomes evident that the dominant contributions to the optical potential take place for  $P \lesssim 1.5 \text{ fm}^{-1}$ . The variation of the momentum  $\mathbf{P}$  yields an off-shell sampling of the  $NN$  effective interaction as given by Eq. (3). The most widely used approximation to

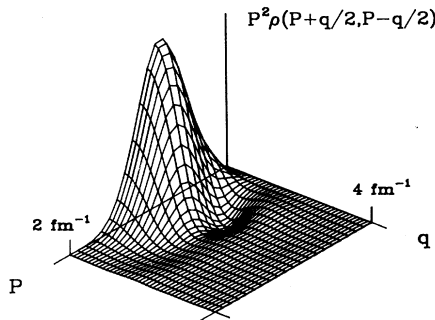


FIG. 1. Mixed density  $\rho(\mathbf{P} + \frac{1}{2}\mathbf{q}, \mathbf{P} - \frac{1}{2}\mathbf{q})$  times  $P^2$  for protons in  $^{40}\text{Ca}$  in arbitrary units.

the full-folding integral is the on-shell  $t\rho$  approximation<sup>8,9</sup> where one assumes, for example, a small variation of the  $t$  matrix in the vicinity of  $\mathbf{P}=0$  and an approximately local behavior in the small- $q$  region. In this case, the optical potential takes the form  $U \sim t(q)\rho(q)$  with the  $t$  matrix always evaluated on shell. Here we present calculations of the optical potential using both the full-folding model and an on-shell  $t\rho$  approximation to it at 200, 300, and 400 MeV.

In order to illustrate the level of agreement between the different potentials in describing the  $NN$  observables, we show in Fig. 2 the isoscalar ( $\Delta T=0$ ) cross section, analyzing power, and spin-rotation parameter for  $NN$  scattering at nucleon laboratory energies of 210 and 325 MeV using only the central ( $A$ ) and spin-orbit ( $C$ )  $NN$  amplitudes.<sup>8</sup> The isoscalar “observables” are shown because it is this combination of the  $NN$   $t$  matrix which enters the calculation of elastic scattering from nuclei with ground-state isospin equal to zero. Similarly, the  $NN$  cross sections have been calculated as  $|A|^2 + |C|^2$  rather than  $|A|^2 + 2|C|^2$  to more closely represent the weighting appropriate<sup>8</sup> to nucleon-nucleus scattering. In this figure, solid curves represent the Paris potential, dashed curves the Bonn potential, dotted curves the HJ potential, and dash-dotted curves the Melbourne potential. The same scattering “observables” were also calculated using Arndt’s amplitudes<sup>10</sup> obtained from an analysis of  $NN$  scattering data and are represented by the symbol  $\diamond$ . From these figures we observe that the

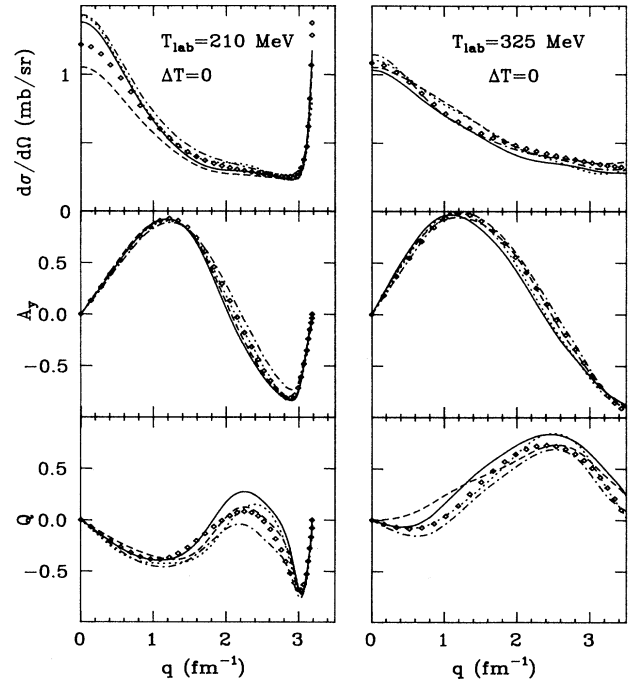


FIG. 2. Calculated cross section, analyzing power, and spin-rotation parameter for  $NN$  scattering ( $\Delta T=0$ ) using different  $NN$  potential models and a phase-shift analysis ( $\diamond$ ) at 210 and 325 MeV lab energy. The solid (Paris), dashed (Bonn), dotted (HJ), and dash-dotted (Melbourne) curves denote results for the different potentials.

different descriptions of the  $NN$  cross sections and spin observables are not completely equivalent. Indeed, in the case of 210 MeV, differences in the cross sections predicted by the four models are quite noticeable. Compared to the predictions from Arndt's phase-shift analysis,<sup>10</sup> the Paris, HJ and Melbourne potentials overestimate the cross section, whereas the Bonn potential underestimates it at small  $q$ . The  $A_y$  and  $Q$  functions are in somewhat closer agreement with each other. In the case of 325-MeV scattering, the dispersion between the predicted  $NN$  cross sections is seen to be smaller than at 210 MeV and each model yields comparable agreement with the predicted observables calculated from the phase-shift analysis.

The above observations regarding the agreement between the different models in describing the  $\Delta T=0$   $NN$  scattering observables are an indication that the  $NN$  potential models are not strictly equivalent on shell. Therefore, applications of these models in full-folding calculations do not permit an unambiguous assessment of the sensitivity of  $NA$  scattering to different off-shell behaviors of  $NN$  potential models. Only in a case in which different  $NN$  potential models provide essentially equivalent descriptions of the  $NN$  data would we be able to explore with confidence their intrinsic differences off shell. Moreover, applications of  $NN$  potentials to the calculation of optical potentials require  $t$  matrices over a wide range of energies in the  $NN$  c.m. This feature precludes a simple analysis of features observed in the calculated  $NA$  scattering observables based on the behavior of the  $NN$  interaction at a particular energy.

To illustrate the variation in the calculated  $NA$  observables associated with on-shell differences in the free  $NN$   $t$  matrices, we show elastic-scattering results in Fig. 3 at 200, 300, and 400 MeV using the conventional  $t\rho$  model for the optical potential which is derived exclusively from on-shell  $t$ -matrix elements as described in Ref. 1. We note that this particular on-shell version of the  $t\rho$  model requires  $t$ -matrix elements at and above the incident energy. Although the comparison between measured and calculated observables is not the primary focus here, we include the data in Fig. 3 to help place the present results in perspective. It is clear that estimates of the effects arising from medium corrections,<sup>11</sup> for example, need to be made, especially at the lower energies. The data at 200 MeV are from Ref. 12. The cross section and  $A_y$  data at 300 and 400 MeV are from Ref. 13; the  $Q$  data at 300 MeV (Ref. 14) correspond to measurements made at 320 MeV.

At 200 MeV we see that the on-shell  $t\rho$  results using the different  $NN$  potentials are in quite close agreement; however, none of these potentials provides a good description of the data. Results using the Bonn potential show the largest deviations from the other  $NN$  potentials as might be expected from the  $NN$  "observables" shown in Fig. 2. At 300 MeV there is a somewhat larger dispersion of the results using the different  $NN$  potentials, especially for the spin observables. As at 200 MeV, the Bonn results exhibit the largest deviation from the mean and provide the best (worst) description of the  $A_y$  (cross section) data. The somewhat distinct results obtained using

the Bonn potential are only partially inferrable from the  $NN$  results of Fig. 2.

For each of the four  $NN$  potential models described above, we have calculated the corresponding free  $t$  matrix fully off shell and then used it in the calculation of full-folding optical potentials for  $p + {}^{40}\text{Ca}$  scattering at 200, 300, and 400 MeV as prescribed by Eqs. (1)–(3). The resulting scattering observables are compared in Fig. 4 where the same convention as that in Fig. 2 is used to represent results for each  $NN$  potential model. From this figure we notice differences between the scattering observables predicted by the four  $NN$  potential models considered. The systematic good agreement observed in the case of the HJ potential at the energies considered here is especially surprising considering the presence of an infinitely strong repulsive core at short distances. In contrast, it is interesting to note the distinct and relatively poor description of the scattering observables obtained using the Melbourne (dot-dashed curves). Indeed, the pronounced improvement obtained in going from the on-shell  $t\rho$  model to the full-folding model when using the Paris, Bonn, and HJ potentials does not occur using the Melbourne potential. These results emphasize that an adequate description of the  $NN$  interaction is not sufficient for describing a many-nucleon process such as  $NA$  scattering. In the case of the two meson-exchange-based potentials (Paris and Bonn), we note a tendency of the Bonn model to yield a slightly more diffractive structure in the cross section, particularly at 200 and 300 MeV as was the case in the on-shell  $t\rho$  results shown in Fig. 3. In the case of the spin observables,  $A_y$  and  $Q$ , the description given by the Bonn potential agrees more closely with the data than that given by the Paris potential. At 400 MeV (Fig. 4), the agreement between the Paris- and Bonn-based calculations is much closer for the cross section, where very good agreement with the data is observed. However, a clear deterioration is observed in the description of  $A_y$  in the case of the Bonn potential, where the minima in  $A_y$  are systematically shallower than those observed in the data.

In summary, the use of the Paris, Bonn, and HJ potential models for the  $NN$  interaction in the calculation of full-folding optical potentials for  $NA$  elastic scattering yields similar overall features for the corresponding scattering observables, especially at the lower incident energies. Although the Melbourne potential provides descriptions of both  $NN$  scattering observables in the  $\Delta T=0$  channel and  $NA$  scattering observables within the on-shell  $t\rho$  model which are comparable to those obtained using the other  $NN$  potentials considered here, its use in full-folding calculations yields a very different (and inferior) description of the corresponding  $NA$  scattering observables. This observation is particularly evident in the analyzing power at all energies considered here and emphasizes the importance of including the off-shell properties of the  $NN$  interaction in as realistic a way as possible. The precise origin of the peculiarities of the Melbourne potential is not investigated in this work. However, previous studies<sup>7</sup> of the properties of the Melbourne potential indicate substantial differences in its off-shell behavior relative to the Paris potential in some

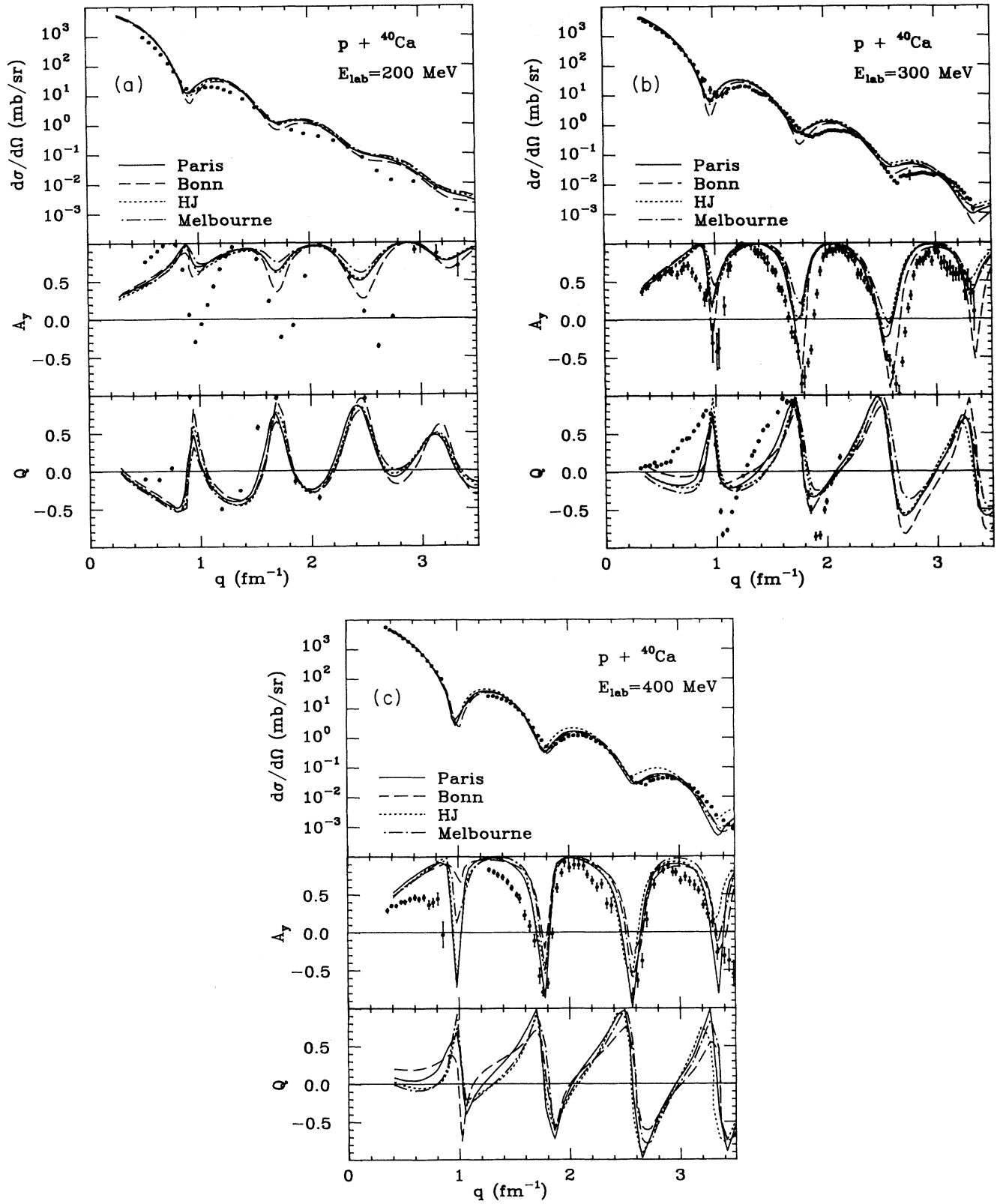


FIG. 3. On-shell  $tp$  calculations of elastic-scattering observables for  $p + {}^{40}\text{Ca}$  at 200, 300, and 400 MeV using the Paris, Bonn, HJ, and Melbourne potentials. The curves are labeled as in Fig. 2.

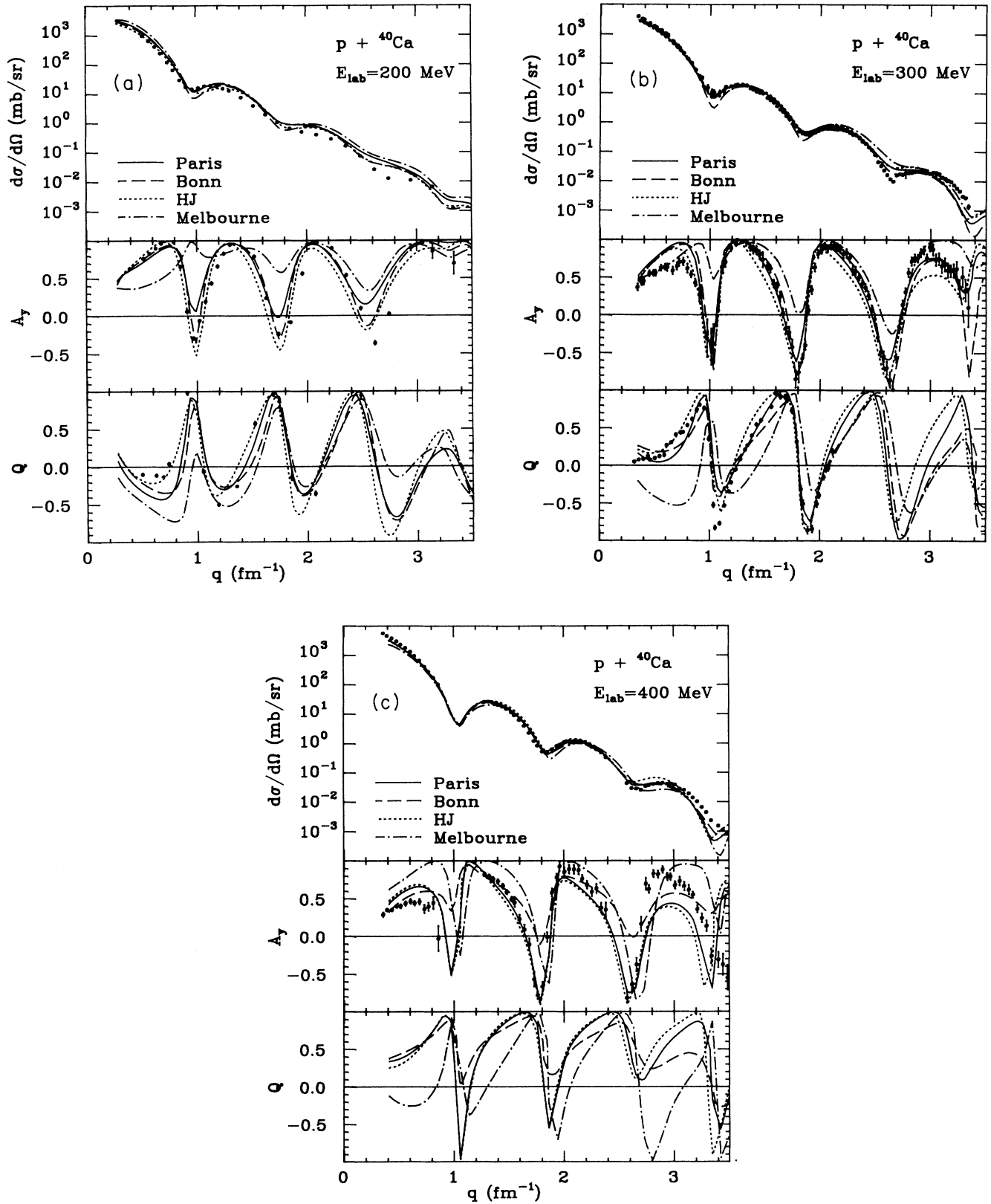


FIG. 4. Full-folding calculations of elastic-scattering observables for  $p + {}^{40}\text{Ca}$  at 200, 300, and 400 MeV using the Paris, Bonn, HJ, and Melbourne potentials. The curves are labeled as in Fig. 2.

channels. In contrast to the results obtained using the Melbourne potential, the much smaller differences found in the calculated observables using the Paris, Bonn, and HJ full-folding results are roughly comparable to those obtained in the corresponding on-shell  $t\rho$  calculations. Consequently, the nonequivalence of the on-shell properties of the different potentials precludes a discrimination amongst these potentials based exclusively on their off-shell extensions. Nevertheless, when used in a full-folding framework, the Paris, Bonn, and HJ potentials provide considerably improved descriptions of the  $NA$

elastic-scattering observables relative to those obtained using the on-shell  $t\rho$  model of the optical potential.

This work was supported in part by National Science Foundation (NSF) Grant PHY-8903856. F. A. B. acknowledges partial support from the Fondo Nacional de Desarrollo Científico y Tecnológico (Chile) Grant No. 1239-90. We also appreciate a grant for computing time provided by the University of Georgia.

<sup>1</sup>H. F. Arellano, F. A. Brieva, and W. G. Love, Phys. Rev. Lett. **63**, 605 (1989); Phys. Rev. C **41**, 2188 (1990); **42**, 652 (1990).

<sup>2</sup>Ch. Elster, Taksu Cheon, Edward Redish, and P. C. Tandy, Phys. Rev. C **41**, 814 (1990).

<sup>3</sup>R. Crespo, R. C. Johnson, and J. A. Tostevin, Phys. Rev. C **41**, 2257 (1990).

<sup>4</sup>M. Lacombe, B. Loiseau, J. M. Richard, R. Vinh Mau, J. Côté, P. Pirès, and R. de Tourreil, Phys. Rev. C **21**, 861 (1980).

<sup>5</sup>R. Machleidt, K. Holinde, and Ch. Elster, Phys. Rep. **149**, 1 (1978); R. Machleidt, in *Advances in Nuclear Physics*, edited by J. Negele and E. Vogt (Plenum, New York, 1989), Vol. 19.

<sup>6</sup>T. Hamada and I. D. Johnston, Nucl. Phys. **34**, 382 (1962).

<sup>7</sup>K. Amos, L. Berge, F. A. Brieva, A. Katsogiannis, L. Petris, and L. Rikus, Phys. Rev. C **37**, 934 (1988).

<sup>8</sup>A. K. Kerman, H. McManus, and R. M. Thaler, Ann. Phys.

(N. Y.) **8**, 551 (1959).

<sup>9</sup>L. Ray and G. W. Hoffmann, Phys. Rev. C **31**, 538 (1985).

<sup>10</sup>R. A. Arndt *et al.*, Phys. Rev. D **28**, 97 (1983); R. A. Arndt and L. D. Roper (unpublished).

<sup>11</sup>H. V. von Geramb, in *The Interaction Between Medium Energy Nucleons in Nuclei, (Indiana Cyclotron Facility, Bloomington, Indiana)*, Proceedings of the workshop on the Interactions Between Medium Energy Nucleons in Nuclei, AIP Conf. Proc. No. 97, edited by H. O. Meyer (AIP, New York, 1982).

<sup>12</sup>E. J. Stephenson, J. Phys. Soc. Jpn. (Suppl.) **55**, 316 (1985).

<sup>13</sup>D. A. Hutcheon *et al.*, Nucl. Phys. **A483**, 429 (1988); P. Schwandt, private communication.

<sup>14</sup>E. Bleszynski *et al.*, Phys. Rev. C **37**, 1527 (1988).